RESEARCH

Size Distributions of Different Orders of Kernels within the Oat Spikelet

Douglas C. Doehlert,* Jean-Luc Jannink, and Michael S. McMullen

ABSTRACT

Oat kernel size uniformity is of interest to the oat milling industry because kernel size is important in the dehulling process. Previous studies indicated that oat kernel size distributions are bimodal. In this study oat spikelets were dissected into primary, secondary, and tertiary kernels and kernel size distributions were determined for each of these kernel orders by digital image analysis. Spikelets with two kernels are the most abundant, and their primary and secondary kernels have distinctly different size distributions. These two kernel spikelets appear to be responsible for the bimodal distribution observed among oat kernels. Primary kernels from single kernel spikelets and primary, secondary, and tertiary kernels from triple kernel spikelets all had different mean sizes and distributions. These kernels appeared to contribute to deviations from bimodal distributions. Thus, data presented provide direct definitive evidence that the non-Gaussian distributions observed for oat kernel sizes are derived from the combination of subpopulations from each of the different orders of kernels from within the spikelet. Sieving analysis of kernel types indicated that for the samples analyzed here, secondary kernels from two kernel spikelets and tertiary kernels from three kernel spikelets appear to contribute equally to undersized kernels under 2 mm in width. Thus, from a kernel size prospective, no advantage can be attributed to the elimination of three kernel spikelets by selective breeding.

D.C. Doehlert, USDA-ARS Hard Red Spring and Durum Wheat Quality Laboratory, Harris Hall, North Dakota State University, Fargo, ND 58105; M. S. McMullen Dep. of Plant Sciences, Loftsgard Hall, North Dakota State University, Fargo, ND 58105; J.-L. Jannink, USDA-ARS Plant Soil and Nutrition Laboratory, Bradfield Hall, Cornell University, Ithaca, NY 14853. Received 9 July 2007. *Corresponding author (douglas.doehlert@ndsu.edu). The mention of firm names or trade products does not imply that they are endorsed or recommended by the U.S. Department of Agriculture over other firms or similar products not mentioned.

Abbreviations: BLUP, best linear unbiased predictor; DIA, digital image analysis; D1, primary kernel from two-kernel spikelet; D2, secondary kernel from two-kernel spikelet; Probl, probability of belonging to subpopulation 1; S1, primary kernel from single kernel spikelet; T1, primary kernel from three-kernel spikelet; T2, secondary kernel from three-kernel spikelet; T3, tertiary kernel from three kernel spikelet.

Oat kernel size distribution is of interest to the oat milling industry because of the role that kernel size has in the dehulling process. Different sizes of oat dehull optimally at different rotor speeds of the impact dehuller used by the oat industry. Oat mills generally separate grain into streams of more uniformly-sized kernels to optimize dehulling efficiency and mill yield (Deane and Commers, 1986; Ganssmann and Vorwerck, 1995). The development of digital image analysis (DIA) has expedited the analysis of oat kernel size by allowing the automated measurement of large numbers of kernels from a single sample (Symons and Fulcher, 1988). Our previous studies using DIA have indicated that oat size distributions usually fit a bimodal model better than a normal distribution (Doehlert et al., 2004; 2005). We have suggested this bimodal distribution might be attributed to the architecture of the oat spikelet.

Published in Crop Sci. 48:298–304 (2008).
doi: 10.2135/cropsci2007.01.0016

677 S. Segoe Rd., Madison, WI 53711 USA

The oat spikelet contains one, two, or three kernels. Double kernel spikelets usually comprise about 80% of the spikelets (Takeda and Frey, 1980; Doehlert et al., 2002). The primary kernel of the spikelet is distinctly larger than the secondary kernel (Schneider, 1912; Zade, 1915; Berry, 1920; Mader, 1927; Milatz, 1933; Villers, 1935; Hutchinson et al., 1952; Youngs and Shands, 1974; Doehlert et al., 2002; Doehlert et al., 2005). We have suggested that the preponderance of two-kernel spikelets has led to the bimodal kernel size distributions, where primary kernels from the two-kernel spikelets make up the larger kernel subpopulation and the secondary kernels make up the smaller kernel subpopulation. The presence of single and triple kernel spikelets were presumed to contribute to departures from the bimodal distribution (Doehlert et al., 2005). Although we have reported correlative data that supports this hypothesis, we have not yet reported direct measurements of kernel size distributions among different oat kernel orders. We have developed a bimodal statistical analysis to facilitate the analysis of oat kernel size distributions (Doehlert et al., 2004). This analysis fits the kernel size distributions into two normally distributed subpopulations and compares the likelihood that the distributions better fit a single normally distributed population or two normally distributed populations. It generates a probability that the distribution is better described by a bimodal model and provides an estimation of the relative size of one putative subpopulation to the other. It also provides estimations of the mean size and variances of each subpopulation. Comparison of distributions generated by the bimodal analysis closely matched the actual distributions (Doehlert et al., 2005).

Some commercial interests discourage the production of cultivars with high frequencies of triple kernel spikelets because of potential contribution of the tertiary kernels to the thin (less than 2 mm wide) kernel fraction, which cannot be processed. However, our analyses (Doehlert et al., 2005) have indicated no correlation among genotypes between triple kernel spikelet frequency and percentage of thin kernels. Also, among environments, there was a negative correlation between triple kernel spikelet frequency and percentage of thin kernels. It appeared that secondary kernels from double kernel spikelets contributed at least as much as tertiary kernels to the thin kernel fraction, and environments that generated more tertiary kernels also generated larger kernels overall. In this study, where we actually isolated the different kernel types, we sought to determine directly the contribution of the different kernel types to the thin kernel fraction.

The main objective in this study was to measure the size distributions of kernels of different orders within the oat spikelet to test the hypothesis that the bimodal distributions of oat kernel size are derived from subpopulations of primary and secondary kernels from double kernel spikelets. We accomplished this by the dissection of oat spikelets and directly measuring the size of the different kernel types. We also modified the bimodal analysis so that it could identify a Prob1 value for each kernel type, allowing unambiguous identification of the composition of the two oat kernel subpopulations. We also tested size distributions of these different kernel classes by using a slotted sieve fractionation to determine the contribution of the different kernel types to the thin kernel fraction to test the hypothesis that tertiary kernels are not the primary source of thin kernels in an oat sample.

MATERIALS AND METHODS

Plant Material

Six genotypes of oat (*Avena sativa* L.) were used for this study including the cultivar Morton, and the breeding lines ND020118, ND020220, ND020247, ND020371, and ND020440. These genotypes were grown in four environments in North Dakota (Carrington, Casselton, Edgeley, and Fargo) in 2004 using three replicate plots per location. A seeding rate of 2.47×10^6 kernels ha^{-1} was used for all experiments. Herbicide treatments were pre-emergence application of 3.93 kg ha^{-1} propachlor and at the 3-leaf stage an application of 0.14 kg ha^{-1} thifensulfuron, 0.07 kg ha^{-1} tribenuron and 0.14 kg ha^{-1} clopyralid. Experimental units were four 2.4-m rows spaced 0.3 m apart. The two center rows were harvested with a two-row binder and threshed with a plot thresher. The harvested grain was cleaned using a Clipper (Bluffton, IN) Model 400 Office Tester and Cleaner fitted with a 4.75 × 19-mm oblong hole sieve and with aspiration adjusted so that kernels containing groats were not removed. The sieve allowed all grain to pass through. Ten panicles were randomly removed from bundles for spikelet analysis.

Panicle and Spikelet Analysis

Panicle and spikelet structures were analyzed by hand dissection. Initially all spikelets were stripped from the panicle and were sorted according to the number of kernels each contained. Then spikelets were dissected and for each spikelet type, kernels were sorted according to their order, and weighed. Thus, data for six kernel types were gathered, these being the primary kernel from a single kernel spikelet (S1), the primary kernel from a two-kernel spikelet (D1), secondary kernel from a two-kernel spikelet (D2), the primary kernel from a three-kernel spikelet (T1), the secondary kernel from a three-kernel spikelet (T2), and the tertiary kernel from a three kernel spikelet (T3). From these data, spikelets per panicle, kernels per panicle, grain mass per panicle, mean mass per kernel, spikelet type frequencies, and mean masses of different order kernels from each spikelet type were recorded. Calculation of these values is described in detail in Doehlert et al. (2002).

Digital Image Analysis

Kernel size was evaluated by digital image analysis. For each sample of ten panicles, kernels of each of the six types were pooled. Entire samples were then photographed. If there were more then ten grams of kernels in a sample, as was the case with some D1 samples, the sample was divided into two photographs. The protocols for photography and analysis were largely identical to those

described by Doehlert et al. (2004), except a digital camera was used instead of an analog (film) camera. The five megapixel images were directly processed by photo editing software (Adobe Photoshop, San Jose, CA). Images were analyzed by the same Amphilion (Amerinex Applied Imaging, Amherst, MA) software described in Doehlert et al. (2004) to measure length, width and image area.

Bimodal Analysis

Kernel image size data from each kernel type dissected from the ten panicles were pooled into a data set, retaining the kernel type and the kernel size information. Pooled data sets contained information from 600 to 1000 kernels. Bimodal analysis was performed as described in Doehlert et al. (2004). The program analyzed the kernel distribution of the kernel sizes and calculated the likelihood that the distributions would be best described by a bimodal model or a normal distribution. It calculated means and variances for kernel sizes within each putative subpopulation, a Prob1 value that was the probability that a particular kernel would be in subpopulation 1 (the subpopulation with the smaller mean), and finally, a bimodal coefficient. Bimodal coefficients larger than 8.0 indicated that the distribution under analysis was significantly better described by the bimodal model rather than a normal distribution.

Two modifications were made to the expectation maximization procedure described in Doehlert et al. (2004). First, in Doehlert et al. (2004), Prob1 was constrained such that $0.10 < \text{Prob1} < 0.90$. Here we narrowed the constraint slightly with $0.15 < \text{Prob1} < 0.85$. In the absence of this constraint, in a minority of cases the analysis took as subpopulation 1 a small set of T3 kernels whereas in the majority of cases subpopulation 1 was dominated by D2 kernels. With the constraint, subpopulation 1 was always dominated by D2 kernels. Thus the constraint ensured that subpopulation 1 had a consistent biological interpretation across all plots. Second, the program was modified to calculate the probability that each observed kernel belonged to subpopulation 1, conditional on its size. For kernel i this probability is denoted p_{1i} and is calculated by applying Bayes' theorem,

$$p_{1i} = \frac{\text{Prob1} \times f(\gamma_i | P_1)}{f(\gamma_i)}$$

$$f(\gamma_i) = \text{Prob1} \times f(\gamma_i | P_1) + (1 - \text{Prob1}) \times f(\gamma_i | P_2)$$

where γ_i is the observation for kernel i and $f(\gamma_i|\mathrm{P}_j)$ is the normal density function for γ_i conditional on the kernel i belonging to subpopulation j. To calculate the probability that a given kernel type could be found in subpopulation 1, the p_{1i} were averaged over all kernels of that type.

Proportions of subpopulation1 represented by specific kernel types were calculated by multiplying the Prob1 for that kernel type by the proportion of that kernel type in the entire population, dividing that value by the Prob1 for the entire sample, expressing the proportion as a percentage. The composition of subpopulation 2 was calculated by an identical procedure, substituting Prob2 for Prob1, where Prob2 was 1 minus Prob1.

Sieving Analysis

Kernel type preparations (from panicle dissections) from each were fractionated into size fractions with slotted sieves and a sizer-shaker (Seedburo Company, Chicago IL). Grain samples were sieved sequentially on slotted 2.58, 2.38, and 1.98-mm sieves. All slots were 19.05 mm long. Grains held back by these sieves were labeled as large, medium, and small, respectively. Kernels that passed through the 1.98-mm sieve were labeled as thin. Data are expressed as mass proportion of the entire sample (summation of all size fractions and kernel types).

Experimental Design and Statistical Analysis

Within each of the four environments, field plots were arranged in a randomized complete block design with three replicates. In the analysis of variance, environments, genotypes, their interaction, and replication were considered random. The genotype × environment interaction was used as the error term for testing the genotype effect and the residual error was used to test the genotype × environment interaction. Best linear unbiased predictors (BLUP) of genotype and environment effects were calculated and are presented augmented by the grand mean of the measurement in question. The least significant difference between BLUP was calculated on the basis of the BLUP standard error. In analyses where kernel type was considered a treatment, the kernel type × environment interaction was used as the error term for testing the effect of kernel type. These statistical analyses, as well as calculation of frequency distributions, means, variances, and coefficients of variation (CV) were performed with the JMP statistical software package (SAS Institute, Cary, NC).

RESULTS AND DISCUSSION

Variation in panicle characteristics for the six genotypes used in this study are shown to demonstrate the behavior of these genotypes in these environments (Table 1). Morton, and ND020371 had more spikelets per panicle than other genotypes and ND020220, ND0200247 and ND020440 had the fewest. Morton, ND020118, and ND02371 had more kernels per panicle than other genotypes and ND020220, ND020247, and ND020440 had the fewest. ND020118 kernels had the greatest mass, whereas Morton, ND020247, ND020371, and ND020440 had the least mass. Morton and ND020371 showed a low frequency of triple kernel spikelets, whereas ND020118 and ND020247 had high triple kernel spikelet frequencies.

Location BLUPs of panicle characteristics (Table 2) indicated significant environmental variation in spikelets per panicle, kernels per panicle, and mean kernel mass, but not in grain mass per panicle. Carrington had the highest triple kernel spikelet frequency. Carrington and Casselton had the highest mean kernel mass. Although data on panicle characteristics have been presented previously (Doehlert et al., 2002), these results are shown to provide essential background to the effects of kernel type frequencies to kernel size distributions of these genotypes in specific environments. Significant genotype × location interactions were observed for spikelets per panicle, grain mass per panicle, percent single kernel spikelets, and

Table 1. Best linear unbiased predictors of panicle characteristics of six oat genotypes grown in replicated plots at four locations in North Dakota in 2004.

Genotype	Spikelet per panicle†	Kernels per panicle	Mean kernel mass	Mass per panicle	Percent single spikelets	Percent double spikelets	Percent triple spikelets
			mg	g	%	%	%
Morton	50.6 ab	92.2 a	34.2 c	3.15 bc	18.7 a	78.6 b	1.7 d
ND020118	45.8 bc	92.2 a	40.3 a	3.68 a	13.5 b	73.7 b	14.0 ab
ND020220	39.0 d	73.4 b	37.6 b	2.76 cd	19.4 a	72.2 b	8.3 bc
ND020247	39.1 d	78.6 b	34.5 c	2.71 d	13.8 b	73.2 b	14.3 a
ND020371	52.2 a	98.6 a	34.5 c	3.40 ab	13.0 b	85.3 a	1.1 d
ND020440	40.5 cd	74.6 b	35.4 bc	2.65 d	19.7 a	74.9 b	4.6 cd

†Values with the same letter in the same column do not differ significantly at $P < 0.05$ (BLUP separation by least significant difference).

Table 2. Best linear unbiased predictors of panicle characteristics of six oat genotypes grown in replicated plots at four locations in North Dakota in 2004.

Location	Spikelet per panicle†	Kernels per panicle	Mean kernel mass	Mass per panicle‡	Percent single spikelets	Percent double spikelets	Percent triple spikelets
			mg	g	%	%	%
Carrington	43.0 b	82.6 b	37.6 a	3.06 a	18.8 a	68.9 b	10.2 a
Casselton	43.6 b	83.8 ab	37.1 a	3.06 a	15.4 ab	77.5 a	7.4 ab
Edgeley	45.1 ab	84.8 ab	34.9 b	3.06 a	18.0 a	76.2 a	5.8 b
Fargo	46.4 a	88.5 a	34.8 b	3.06 a	13.2 b	82.7 a	5.9 b

†Values with the same letter in the same column do not differ significantly at $P < 0.05$ (BLUP separation by least significant difference).

‡No variance among locations was found for mass per panicle, so the best predictor for all locations is the grand mean.

percent double kernel spikelets. The interactions appear derived from differences in magnitude of responses of genotypes in different environments.

Grand means of kernel type mass, frequency, and kernel linear dimensions for the six genotypes across four environments are shown in Table 3. As observed previously (Takeda and Frey, 1980; Doehlert et al., 2002; Doehlert et al., 2005), kernels from double kernel spikelets were the most abundant, expressed either according to number or mass. Rankings of kernel types according to kernel mass were largely consistent with the ranking according to linear measures, including area, length and width (Table 3). Bimodal analysis was modified to calculate the probability that any particular kernel would be in subpopulation 1 of the two subpopulations postulated by the statistical analysis (Table 3). This is the subpopulation with smaller kernel size. Calculations based on values in Table 3 suggested that 69.7% of subpopulation 1 was composed of D2 kernels, 12.0% was D1 kernels, 5.9% was S1 kernels, 0.7% was T1 kernels, 5.0% was T2 kernels, and 6.9% was T3 kernels. Subpopulation 2 was composed of 77.4% D1 kernels, 0.9% D2 kernels, 12.7% S1 kernels, 7.5% T1 kernels, 1.8% T2, kernels and 0% T3 kernels.

The bimodal distribution can be better visualized by graphical analysis of the distributions of the different kernel types. We present three examples to represent our

Table 3. Mass and linear dimensions of kernel types from six oat genotypes grown in replicated plots at four locations in North Dakota in 2004. Values are means pooled from all replicates, genotypes and locations. Kernel linear size was determined by digital image analysis.

Kernel type†	Percent by number‡	Percent by mass	Prob 1§	Kernel mass	Kernel area	Kernel length	Kernel width
	%	%		mg	mm^2	mm	mm
Mean			0.57 c	36.1 d	23.5 d	11.6 d	2.96 e
D1	40.1 a	49.2 a	0.17 e	44.3 b	28.6 b	13.0 b	3.14 b
D2	40.1 a	31.6 b	0.99 a	28.5 e	18.3 f	10.1 f	2.77 d
S1	8.8 b	9.5 c	0.38 d	38.9 c	27.1 c	12.5 c	3.14 b
T1	3.6 c	4.9 d	0.11 f	50.9 a	32.4 a	13.7 a	3.29 a
T2	3.6 c	3.5 d	0.79 b	35.6 d	22.7 e	11.2 e	3.03 c
T3	3.6 c	1.2 e	1.00 a	13.0 f	10.7 g	7.3 g	2.17 f

†D1 primary kernel from double kernel spikelet, D2 secondary kernel from double kernel spikelet, S1 primary kernel from single kernel spikelet, T1 primary kernel from triple kernel spikelet, T2 secondary kernel from triple kernel spikelet, T3 tertiary kernel from triple kernel spikelet.

‡Values with the same letter in the same column do not differ significantly at $P < 0.05$ (mean separation by least significant difference).

§The probability that kernels of this type will fall within subpopulation 1, as defined by the bimodal model.

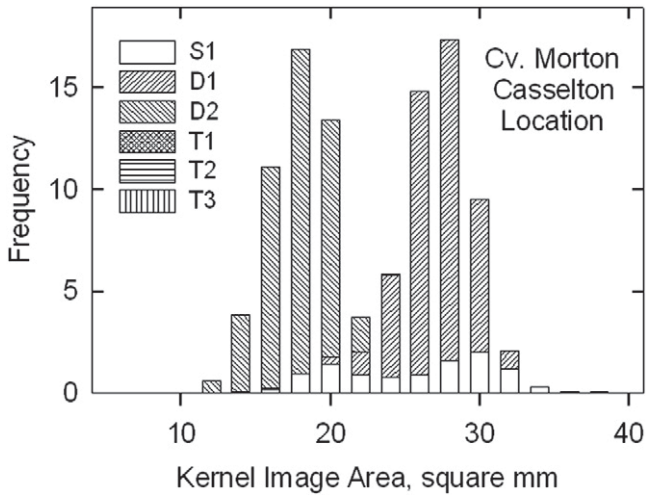

Figure 1. Size distributions of kernel types of Morton oat grown in Casselton, ND in 2004. S1, primary kernels from single kernel spikelets; D1, primary kernel from two-kernel spikelet; D2, secondary kernel from two kernel spikelet; T1, primary kernel from triple kernel spikelet; T2, secondary kernel from triple-kernel spikelet; T3, tertiary kernel from triple kernel spikelet.

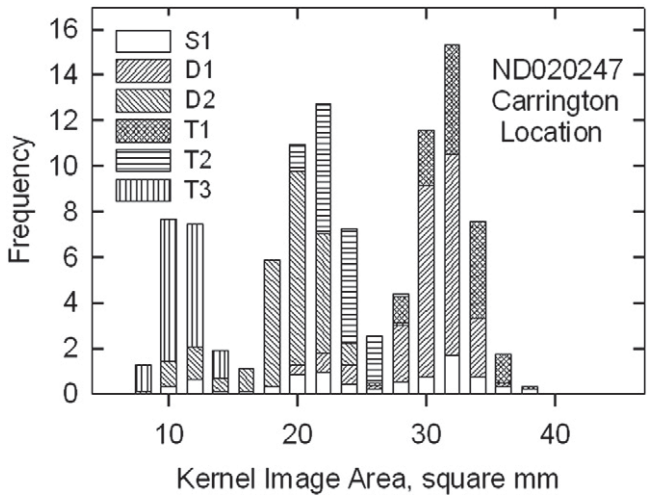

Figure 2. Size distributions of kernel types of ND020247 oat grown in Carrington, ND in 2004. S1, primary kernels from single kernel spikelets; D1, primary kernel from two-kernel spikelet; D2, secondary kernel from two kernel spikelet; T1, primary kernel from triple kernel spikelet; T2, secondary kernel from triple-kernel spikelet; T3, tertiary kernel from triple kernel spikelet.

data. The first example is of Morton oat from Casselton (Fig. 1), which represents a low triple kernel genotype at a low triple kernel environment. This example is extreme in that there were no triple kernel spikelets in this sample. The bimodal pattern is very clear. The D2 kernels appear to be confined to the mode containing the smaller sized kernels, or what would be designated subpopulation 1 by the bimodal analysis. There is some overlap of D1 kernels into this subpopulation, although most of the D1 kernels fall into what we would visually consider to be subpopulation 2. More S1 kernels appear to fall into subpopulation 2 than subpopulation 1.

The second example represents another extreme, ND020247 from Carrington, where triple kernel spikelets were relatively abundant (Fig. 2). This distribution appears distinctly trimodal, where a third mode appears to be associated with the T3 kernels. The bimodal analysis occasionally identified the T3 mode as population 1 in samples with high frequencies of triple kernel spikelets. We avoided this problem by stipulating within the program a minimum value of Prob1 of 0.15. This would require that subpopulation 1 contained more than 15% of the total kernels in the sample and resulted in subpopulation 1 being primarily comprised of D2 kernels. Although T3 kernels are abundant in number in this figure, they represented a small proportion of the sample by mass. The T2 kernels contributed strongly to the distribution of subpopulation 1, and shifted the mode toward a value larger than the mean size of the D2 kernels. The T1 kernels contributed to subpopulation 2 and presumably shifted the mean kernel size of subpopulation 2 to a value larger than the mean of the D1 kernels.

The third example we present is the grand mean of all genotypes from all environments (Fig. 3). The pattern of the distribution appeared bimodal. As indicated by the numerical distributions (Table 3) the distribution of S1 kernels was spread widely, but fell mostly in the range of the subpopulation 2 (larger kernels). The D1 kernels were primarily with subpopulation 2 (larger kernels), and the D2 kernels were distinctly in the subpopulation 1 (smaller kernels). The T1 kernels were mostly distributed on the larger side of the subpopulation 2 mode. The T2 kernels fell mostly in between the two modes, but a larger proportion fell within subpopulation 1. The T3 kernels appeared to form an additional mode smaller than subpopulation 1.

Among these distributions (Fig. 1, 2, 3), S1 kernel distributions appear somewhat multi-modal among themselves. Takeda and Frey (1980) used a more discriminatory segregation of kernel classes than used here, and identified kernels from single kernel spikelets as being derived from a primary floret, a secondary, or even a tertiary floret, where other florets in the spikelet abort. Results of Rajala and Peltonen-Sainio (2004) indicated that the cell number is greater in primary kernels than in secondary kernels, so that the potential size of a kernel may be predetermined by cell number according to kernel order. Perhaps the multi-modal distribution of S1 kernels stems from their derivation from different orders of kernels.

Because high proportions of thin oat kernels are often attributed to high tertiary kernel frequency, we subjected the different kernel types to sieving analysis (Table 4). Although about half of the T3 kernels were thins, the T3 kernels accounted for less than half of the total thin kernels. The D2 kernel type comprised 46.9% of the undersized kernels. D1 and T2 kernels also contributed to undersized kernels, but to lesser extents. The total proportion of undersized kernel was less than 2%

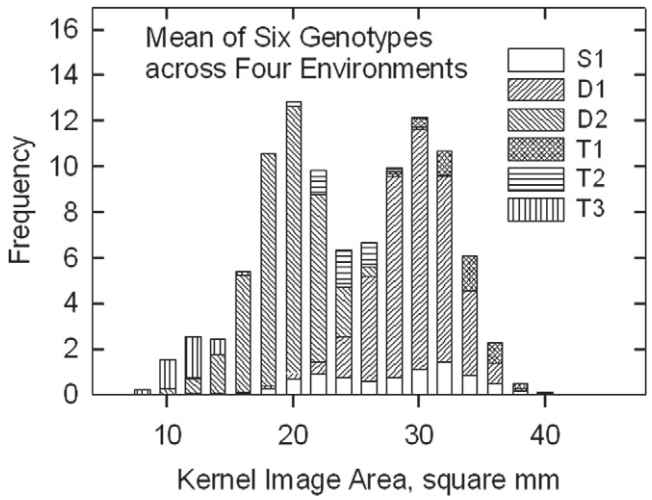

Figure 3. Size distributions of kernel types of six genotypes of oat grown in four environments in 2004. S1, primary kernels from single kernel spikelets; D1, primary kernel from two-kernel spikelet; D2, secondary kernel from two kernel spikelet; T1, primary kernel from triple kernel spikelet; T2, secondary kernel from triple-kernel spikelet; T3, tertiary kernel from triple kernel spikelet.

of the total, which is low. The field conditions in which these plots were grown were particularly favorable for producing high quality grain and thus a relatively low proportion of undersized kernels was observed. Past experience (Doehlert et al., 2002) has suggested that poorer growth conditions would generate more undersized kernels and less triple kernel spikelets. This would result in a much higher relative contribution of D2 kernels to the undersized kernel pool. Results reported here reinforce conclusions from Doehlert et al. (2002) that D2 kernels contribute at least as much to undersized kernels as do T3 kernels. Thus, we see no advandage from a kernel size prospective, from the elimination of triple kernel spikelets by selective breeding.

We compared the mean kernel size of the subpopulation 1 and subpopulation 2 kernels as measured by kernel image area with the mean kernel areas of D1 and D2 kernels (Table 5) for this data set. Here we sought to determine how well the bimodal analysis predicted the mean sizes of D1 and D2 kernels. For kernel area, D1 kernels had mean area of 28.6 mm^2, whereas subpopulation 2 had a mean area of 29.5 mm^2. These values differ by less than 1 mm^2, which could be considered a small difference, however, a paired *t* test indicated that this was a significant difference. Similarly, even though the difference between the mean image area of D2 kernels and subpopulation 1 was only 0.7 mm^2, this difference was significant by *t* test. Similarly, small but significant differences were observed in length between D1 and subpopulation 2, and D2 and subpopulation 1. The width of D2 kernels did not differ significantly from the width of subpopulation 2 kernels, although the width of D1 kernels width differed significantly from subpopulation 1 kernels (Table 5). Thus, sizes of kernels from subpopulations 1 and 2 appear to correspond well with sizes of D2 and D1 kernels. Breeding efforts to improve oat kernel size uniformity could possibly use the bimodal analysis to select for lines with reduced size differences between D1 and D2 kernels.

The results presented here directly show that the bimodal distribution of oat kernel sizes can be attributed to subpopulations of primary and secondary kernels from double-kernel oat spikelets. The primary kernels from these spikelets clearly make up most of the larger sized kernels of the subpopulation 2, and the smaller secondary kernels constitute most of the kernels of subpopulation 1 (Table 2, 3, Fig. 1, 2, 3). The distributions of S1, T1, T2, and T3 kernels, as seen in Fig. 2, illustrate how the presence of single and triple kernel spikelets can influence the bimodal distribution. The T1 kernels were the largest and fell on the large side of subpopulation 2, skewing that peak toward the larger size. The T2 kernels often fell between the two major modes, which diminished the distinctiveness of both. The T3 kernels tended to form a

Table 4. Kernel type composition of different oat kernel size fractions generated by sequential sieving. Large kernels (32.3% of total mass) were held back by 2.58 mm slots. Medium kernels (38.3% of total mass) were held back by 2.38 mm slots. Small kernels (27.6% of total mass) were held back by 1.98 mm slots. Thin kernels (1.65% of total mass) passed through the 1.98 mm slot.

Type†	% Large‡	% Medium	% Small	% Thins
D1	43.6 a	52.8 a	40.5 a	7.2 b
D2	22.2 b	29.9 b	42.4 a	46.9 a
S1	23.6 b	7.0 c	4.9 b	0.6 b
T1	7.7 c	4.9 c	1.8 b	0.1 b
T2	3.0 d	4.8 c	3.0 b	1.0 b
T3	0.0 d	0.5 d	7.4 b	44.3 a

†D1 primary kernel from double kernel spikelet, D2 secondary kernel from double kernel spikelet, S1 primary kernel from single kernel spikelet, T1 primary kernel from triple kernel spikelet, T2 secondary kernel from triple kernel spikelet, T3 tertiary kernel from triple kernel spikelet.

‡Values with the same letter in the same column do not differ significantly at $P < 0.05$ (mean separation by least significant difference).

Table 5. Comparison of mean dimensions of D1 kernels (primary kernels from double kernel spikelets) with those of subpopulation 2 as determined by bimodal analysis, and the dimensions of D2 kernels (secondary kernels from double kernel spikelets) with subpopulation 1, also determined by bimodal analysis (n = 450).

	Area	Length	Width
	mm^2	mm	mm
D1	28.6	13.2	3.20
Subpopulation 2	29.5	13.0	3.14
Paired *t* test	**	**	**
D2	18.3	10.3	2.78
Subpopulation 1	19.0	10.1	2.77
Paired *t* test	**	**	NS

**values differ significantly, $P < 0.01$

NS, not significant.

separate smaller mode distinct from that of the D2 kernels, which was incorporated into subpopulation 1 by the bimodal analysis performed in this study.

The data that were gathered in this experiment allowed us to test how well mean D1 and D2 kernel sizes were predicted by the bimodal model (Table 5). We found that D1 and D2 kernel sizes were predicted within 5% of their measured sizes. The bimodal analysis usually predicted larger means than were actually observed. Graphical analysis would suggest that this shift was due to kernels from triple kernel spikelets. Although these might be considered to be good predictive values for these kernel sizes, the predicted values differed statistically (by paired *t* test) from the independently measured values. Our experience has suggested that prediction of D1 and D2 kernel size from DIA data is less time consuming than direct measurement by spikelet dissection. Thus, such predicted values may be of considerable value to efforts attempting to improve kernel size uniformity by reducing the size differences between D1 and D2 kernels.

CONCLUSIONS

The bimodal oat kernel size distribution is attributed to the primary and secondary kernels of the double kernel spikelet. Deviations from the bimodal distribution can be attributed to single and, more importantly, triple kernel spikelets. Although T3 kernels were largely undersized for milling purposes, they comprised less than half of all undersized kernels. The D2 kernels contributed as much to undersized kernels as did T3 kernels.

References

Berry, R.A. 1920. Composition and properties of oat grain and straw. J. Agric. Sci. 10:360–414.

Deane, D., and E. Commers. 1986. Oat cleaning and processing. p. 371–412. *In* F.H. Webster (ed.) Oats: Chemistry and technology. American Association of Cereal Chemists, St. Paul, MN.

Doehlert, D.C., M.S. McMullen, J.-L. Jannink, S. Panigrahi, H. Gu, and N.R. Riveland. 2004. Evaluation of oat kernel size uniformity. Crop Sci. 44:1178–1186.

Doehlert, D.C., M.S. McMullen, J.-L. Jannink, S. Panigrahi, H. Gu, and N.R. Riveland. 2005. A bimodal model for oat kernel size distributions. Can. J. Plant Sci. 85:317–326.

Doehlert, D.C., M.S. McMullen, and N.R. Riveland. 2002. Sources of variation in kernel size in oats. Cereal Chem. 79:528–534.

Ganssmann, W., and K. Vorwerck. 1995. Oat milling, processing and storage. p. 369–408. *In* R.W. Welch (ed.) The oat crop: Production and utilization. Chapman & Hall, London.

Hutchinson, J.B., N.L. Kent, and H.F. Martin. 1952. The kernel content of oats: Variation in percentage kernel content and 1000 kernel weight within the variety. J. Natl. Inst. Agric. Bot. 6:149–160.

Mader, W. 1927. Zur Frage der Bestimmung des 1000-Korngewichtes zur sortencharakteristik bei Hafer. Fortschr. Landw. 2:550–552.

Milatz, R. 1933. Neue Hafersortenmerkmale. Angew. Bot. 15:481–518.

Rajala, A., and P. Peltonen-Sainio. 2004. Intra-plant variation for progress of cell division in developing oat grains: A preliminary study. Agric. Food Sci. 13:163–169.

Schneider, G. 1912. Vegetationsversuche mit 88 Hafersorten. Landwirtsn. Jahrb. 42:767–833.

Symons, S.J., and R.G. Fulcher. 1988. Determination of variation in oat kernel morphology by digital image analysis. J. Cereal Sci. 7:219–228.

Takeda, K., and K.J. Frey. 1980. Tertiary seed set in oat cultivars. Crop Sci. 20:771–774.

Villers, P.J.R.J. 1935. A genetic study of the inheritance of various characters in certain *Avena* hybrids. Bull. Dep. Agric. Stellenbosch S. Afr. Sci. 140:90.

Youngs, V.L., and H.L. Shands. 1974. Variation in oat kernel characteristics within the panicle. Crop Sci. 14:578–580.

Zade, A. 1915. Methoden zur Bestimmung des Spelzenanteils beim Hafer. Fuhlings Landw. Z. 64:295–311.